Mar Geophys Res (2011) 32:493–501
DOI 10.1007/s11001-011-9141-1

ORIGINAL RESEARCH PAPER

Gridding heterogeneous bathymetric data sets with stacked continuous curvature splines in tension

Benjamin Hell · Martin Jakobsson

Received: 18 May 2011 / Accepted: 18 September 2011 / Published online: 19 October 2011

Abstract Gridding heterogeneous bathymetric data sets for the compilation of Digital bathymetric models (DBMs), poses specific problems when there are extreme variations in source data density. This requires gridding routines capable of subsampling high-resolution source data while preserving as much as possible of the small details, at the same time as interpolating in areas with sparse data without generating gridding artifacts. A frequently used gridding method generalizes bicubic spline interpolation and is known as continuous curvature splines in tension. This method is further enhanced in this article in order to specifically handle heterogeneous bathymetric source data. Our method constructs the final grid through stacking several surfaces of different resolutions, each generated using the splines in tension algorithm. With this approach, the gridding resolution is locally adjusted to the density of the source data set: Areas with high-resolution data are gridded at higher resolution than areas with sparse source data. In comparison with some of the most widely used gridding methods, our approach yields superior DBMs based on heterogeneous bathymetric data sets with regard to preserving small bathymetric details in the high-resolution source data, while minimizing interpolation artifacts in the sparsely data constrained regions. Common problems such as artifacts from ship tracklines are suppressed. Even if our stacked continuous curvature splines in tension gridding algorithm has been specifically designed to construct DBMs from heterogeneous bathymetric source data, it may be used to compile regular grids from other geoscientific measurements.

B. Hell (✉) · M. Jakobsson
Department of Geological Sciences, Stockholm University, 10691 Stockholm, Sweden
e-mail: benjamin.hell@geo.su.se

Keywords Gridding · Interpolation · Digital bathymetric model · Seafloor topography · Bicubic splines in tension

Introduction

Analysis and interpretation of geoscientific data representing some property over a two-dimensional surface is facilitated if the measured variable is evenly distributed on a regularly spaced 2D lattice, henceforth referred to as a grid. Examples include Fourier analysis (Pollard 1971), derivatives of topography such as slope or aspect (Zhou and Liub 2004), and cartographic techniques such as hill shading (Ware 1989). However, many geoscientific field measurements are acquired irrevvvgularly in the 2D space due to constraints regarding for example accessibility, cost and survey time. It is therefore common that the measurements are distributed along survey lines or in clusters over areas of specific interest. The process of estimating values of an arbitrary sampled function at regularly spaced intervals is known as gridding. Gridding is a combination of subsampling, interpolation and sometimes even extrapolation in two dimensions. The basic rationale behind spatial interpolation is spatial autocorrelation (Tobler 1970, often referred to as the "first law of geography"). This concept implies that the values of a function sampled at points close together are more likely to be similar than values of points located further apart. Substantial efforts have been put into processing of geoscientific data sets to obtain gapless, consistent and simple to use gridded data products. For example, the high-resolution grid derived from the Shuttle Radar Topography Mission provides coherent elevation data for most of the Earth's land masses (Farr et al. 2007; Reuter et al. 2007). Other widely used grids assembled from irregularly spaced measurements are

the age of oceanic crust (Müller et al. 2008), the marine gravity anomaly (Sandwell and Smith 1997), and the ocean bathymetry (Smith and Sandwell 1997; Jakobsson et al. 2000, 2008; Becker et al. 2009).

Seafloor depths, bathymetry, have been measured systematically for more than a century (Hall 2006). Over that period, methods and equipment for depth measurements have evolved tremendously, from single lead line depth soundings taking hours to modern multibeam sonars producing hundreds of measurements over the course of some seconds. However, due to the vastness of the world ocean, completely mapping the seafloor with shipboard measurements is still beyond technological feasibility (Vogt et al. 2000). Therefore, most previously acquired, technologically antiquated soundings are still required for regional and global bathymetric compilations. The world ocean bathymetric database is extremely heterogeneous imposing challenges for the compiler(s) of gridded Digital bathymetric models (DBMs).

In this article, we present a novel gridding method, which accounts for the local data density at each grid cell when interpolating bathymetric observations onto a regular 2D lattice. Areas densely covered with data are gridded at higher resolutions than areas with sparse data cover. Our method builds on stacking these multi resolution grids; each generated using the minimum curvature splines in tension gridding algorithm by Smith and Wessel (1990). We evaluate our gridding approach in an area of the Fram Strait, between Svalbard and northeast Greenland that partly has been mapped with multibeam and partly with single beam echo sounders. Our evaluation shows that gridding with stacked continuous curvature splines in tension produces a superior final DBM compared to gridding at one pre-defined resolution using some of the most commonly used gridding algorithms.

Background

Generally, there are two classes of interpolation methods used in gridding; global prediction and local deterministic methods (Burrough and McDonnel 1998, p. 102). Included in global prediction methods are trend surfaces built from regression analysis, which may be justified if the mean and variance of the observations do not vary too much spatially. In other cases, a variance analysis of the data may provide the base for the interpolation method. Kriging is the most common example of such geostatistical method (Matheron 1963; Isaaks and Srivastava 1990). Kriging offers the intriguing possibility of uncertainty estimation, although the method is computationally demanding when applied to very large numbers of observations in combination with long-range spatial autocorrelation (Hartman and Hössjer 2008; Furrer et al. 2006). Therefore, Kriging has mostly been applied to problems dealing with smaller data sets (Haining et al. 2010), and is difficult to apply when gridding large parts of the world ocean involving typically hundreds of millions of data points rather than hundreds of thousands.

One of the most commonly used interpolation algorithm in geoscience is bicubic spline interpolation (Briggs 1974). Through all observations the spline interpolation fits a surface with continuous second derivatives and minimized total squared curvature. The method is exact, implying that observations are exactly reproduced if they coincide with grid nodes. The interpolated surface is therefore smooth, although the minimum curvature constraint may lead to interpolation artifacts in the form of artificial local extreme highs or lows between observations (de Boor 2001). These oscillations are largely dependent on locations and values of the observations, and tend to occur in places where the sampled function features drastic changes and observations are sparse. Smith and Wessel (1990) improved the bicubic spline interpolation algorithm by introducing a tension factor that relaxes the minimum curvature criterion. This greatly reduces the problems with artificial extremes occurring in between the input data points. Smith and Wessel (1990) showed that the computational cost of their algorithm is the same as for conventional spline interpolation. A critical pre-processing step before spline interpolation is subsampling of regions densely covered with observations, because the input observations should only contain information below the Nyquist frequency of the final grid (Smith and Wessel 1990). This is commonly done by applying a block mean or median filter on all the data to be gridded with the same block size as the final grid resolution. Bicubic splines in tension have been used to interpolate several widely used DBMs. One example is the $1^\circ \times 1^\circ$ resolution DBM of the world ocean produced by the General Bathymetric Chart of the Ocean (GEBCO) by gridding the depth contours digitized from the GEBCO charts series (Task group on gridding of the GEBCO SCDB 1997). Another is the International Bathymetric Chart of the Arctic Ocean (IBCAO) compiled from a variety of bathymetric sources including single and multibeam echo soundings, spot observations, and digitized depth contours from published charts (Macnab and Jakobsson 2000; Jakobsson et al. 2008).

A result of the subsampling involved in the preparation of bathymetric data for spline interpolation is that small details present in high-resolution observations are discarded in the gridding process. Usually this happens to dense, modern multibeam data, arguably the highest quality parts of the data set and thus very valuable information. The remove-restore algorithm (Forsberg and Tscherning 1981; Forsberg 1993; Torge 2001) partly accounts for this problem. From each source data point the value of a low

frequency surface at the same place is subtracted. Subsequently, this "reduced" source data set is gridded. The resulting grid of small variations from the low frequency surface is then added to this surface again. In this way the observations are reproduced where they exist and the low-resolution trend surface dominates regions without data support. This method is especially suitable when combining different kinds of data, such as low-resolution satellite altimetry with high-resolution ship soundings when compiling bathymetric data (Becker et al. 2009).

Variable grid cell sizes

The most commonly used DBMs have a constant grid cell size over the entire data set (e.g. Smith and Sandwell 1997; Jakobsson et al. 2008; Becker et al. 2009). The selected grid cell size is a trade-off, although generally decided based on the desired shortest range of small-scale morphological variations that can be reproduced by the source data. Areas featuring a lower level of morphological details or areas with only low-resolution source data are thus usually oversampled. The upsampling causes a number of obvious potential problems: (1) Several of the standard interpolation algorithms do not yield reliable results when interpolating coarse data onto a fine grid. (2) The size of the resulting grid is larger than needed to portray the actual data content. (3) It is not clear from a user perspective whether an area is smooth in reality or because of a lack of data. An approach to adjust the grid cell sizes considering the source data or local circumstances is therefore warranted. In the geosciences, grids with variable cell sizes are commonly used in climate and oceanographic modeling, whereas little work has been done regarding gridding topography or bathymetry with variable cell sizes. One classical approach to variable node spacing is Delaunay triangulation that produces a Triangulated Irregular Network (TIN) of the source data points (Delaunay 1934). However, Delaunay triangulation only connects source data points in an optimal way that maximizes the minimum angle of each triangle. This leads to a triangulated tessellation striving to avoid "skinny" triangles. Delaunay triangulation does neither incorporate interpolation between them, nor the possibility to subsample data.

To determine the optimal local grid resolution, two strategies are obvious. In the first strategy, the local grid resolution is determined by morphology, where areas with short-range spatial autocorrelation and highly variable morphology (e.g. mid ocean ridges) are sampled with higher resolution than relatively flat or smooth areas (e.g. abyssal plains). Such a grid would optimize the number of grid nodes needed to give a portrayal of seafloor morphology as natural as possible. In second strategy, the source data density governs the final grid resolution. In this approach, areas with high-resolution source data are portrayed at high resolution and vice versa. The properties of such a grid reflect the source data density. The gridding method presented in this work involves the second strategy.

Methods

Gridding with stacked continuous curvature splines in tension

The gridding method presented here is based on using interpolation with splines in tension at various resolutions decided according to source data density. The method allows gridding parameters, such as the tension factor, to be adjusted individually for each grid resolution. Each grid is essentially compiled using the same approach as the examples given by Smith and Wessel (1990), however, with some important differences concerning how areas with sparse data are treated.

Prior to computing a grid of a specific resolution, a median value of all source data points is derived for each grid cell using block median filtering. In this preprocessing step different data sets could also be weighted differently, for instance with greater weights for data of higher accuracy. However, in the examples presented below, uniform weights were used.

The filtered source data is gridded in a series of N different resolutions, starting at the highest resolution r and doubling the cell size until a grid without gaps is obtained (Fig. 1a). The resolution thus follows $2^{n-1}\,r$ for $n = 1, 2, \ldots, N$. Each of the grids is set to not-a-number (NaN) values in areas where the source data is not sufficiently dense for the respective resolution (see implementation details below). Subsequently, the grids are stacked onto each other, with higher resolution grid cells overruling lower resolution ones (Fig. 1a). The result is a set of grid nodes with variable spacing. In a final step, these grid nodes may be interpolated once more onto a grid with constant cell size of the highest possible resolution. This last step is optional, although practically essential because most software for grid analysis and visualization only are able to deal with constant grid cell sizes. The variable grid output is therefore of rather limited use at present.

The entire process is based on the open source software Generic Mapping Tools (GMT, Wessel and Smith 1998). The block median filtering is carried out with the GMT program *blockmedian*. The GMT program *surface* was modified to include the possibility of masking out grid cells by setting nodes insufficiently covered by source data to NaN (Fig. 1b). When interpolating a grid node, the spline in tension algorithm implemented in *surface* (Smith and

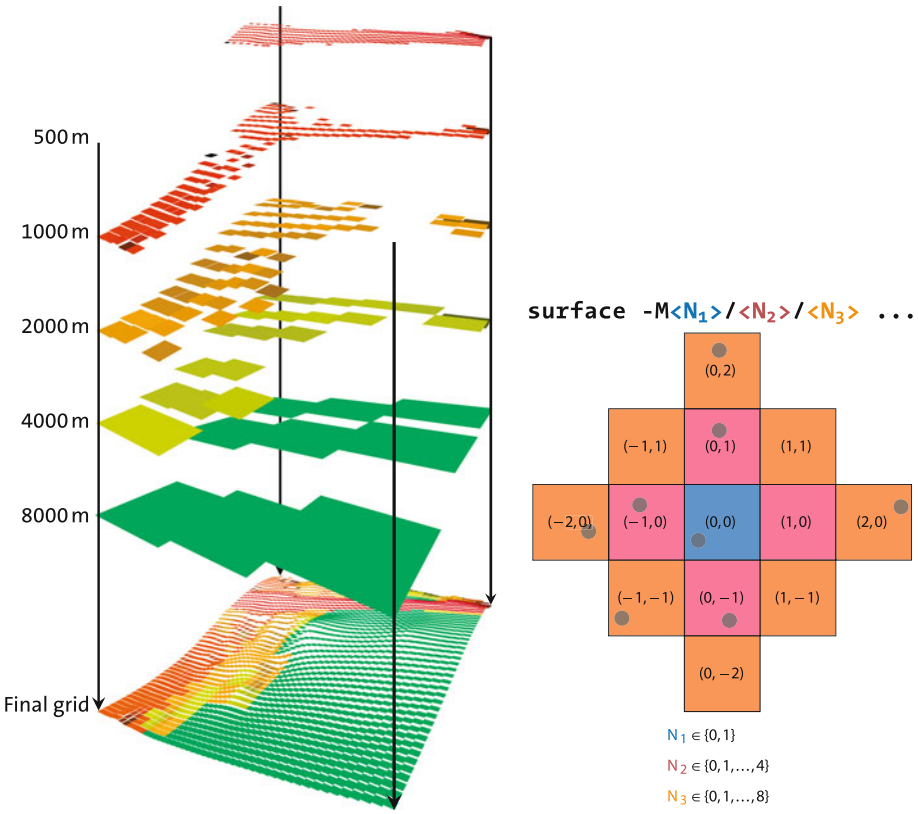

(a) Grid stacking **(b)** Surface masking

Fig. 1 Stacking grids with different resolutions: A series of grids with different resolutions is computed using median block filtering and splines in tension interpolation. After the interpolation, each grid is masked out in areas not sufficiently constrained by the source data. **a** The grids are stacked using the new GMT program *grdstack*. If a grid cell is the highest resolution possible at a specific place, its value is preserved in the final grid. In the example shown, up to 8 km grid cells are needed to close all gaps in the source data. **b** The masking function added to GMT *surface* (figure adopted from Smith and Wessel 1990). The finite difference solution for interpolating the central grid node (0,0) takes the values of data within 13 grid cells into account. Increasing tension increases the weight of the *red grid* cells relative to the orange ones. The masking function implemented in *surface* allows specifying how many grid cells of each sort must be constrained by source data. If this constraint is not fulfilled, the interpolated value of the central cell will be discarded, i.e. set to NaN. In the example shown the default setting of -M1/3/5 is too strict to keep the interpolated value at (0,0). With a setting of e.g. -M1/2/4, the cell would be kept

Wessel 1990) considers data within thirteen grid cells surrounding the interpolated node (Fig. 1b). The *surface* masking functionality added in this work provides a flexible way to specify how many of these cells must be populated with source data in order to keep the interpolated node.

The Generic Mapping Tools offer the possibility to mask grids using the programs *nearneighbor* and *grdmask*, too. However, our tests with these programs instead of the modified *surface* yielded far inferior results. In particular it was difficult to reliably suppress track line artifacts with the radius and sector based approach in *nearneighbor*.

As the grid resolution increases, the area of the named twelve grid cells extends and the data support constraints can be satisfied more easily resulting in fewer gaps in the grid. Lower resolution grids are added to the stack until all gaps are closed. An additional GMT program, *grdstack*, was developed in order to stack all the individually interpolated grids of different resolutions (Fig. 1a).

To fill all data gaps in the data set used for testing (see below), a grid resolution as low as 16,000 m is required. The high-resolution multibeam data warrants a highest resolution of 500 m. According to the relation above, the following intermediate grids were computed before reaching 16,000 m: 1,000, 2,000, 4,000 and 8,000 m. Source data was required in eight of twelve grid cells surrounding the interpolated node, or the node would be masked out (default *surface* masking setting *M1/3/5*). At all resolutions, the data was gridded with a uniform tension factor $T = 0.32$, and after block median filtering the source data accordingly. When the source data density is even more heterogeneous than in the sample data set presented here, our tests have shown that higher tension factors may be beneficial for the coarsest grids.

Study area and bathymetric source data

To evaluate our new gridding approach and compare it with other standard gridding methods, a test data set was assembled from the Fram Strait between Greenland and Svalbard (Fig. 2a). The Fram Strait features a complex bathymetry, including the northern prolongation of the Mid Atlantic Ridge. On this spreading center the Molloy Hole is located; a pull-apart basin and the deepest place in the Arctic Ocean reaching a depth of 5,669 m (Klenke and Schenke 2002). The bathymetric test data were extracted from the database used to compile IBCAO Version 2.0

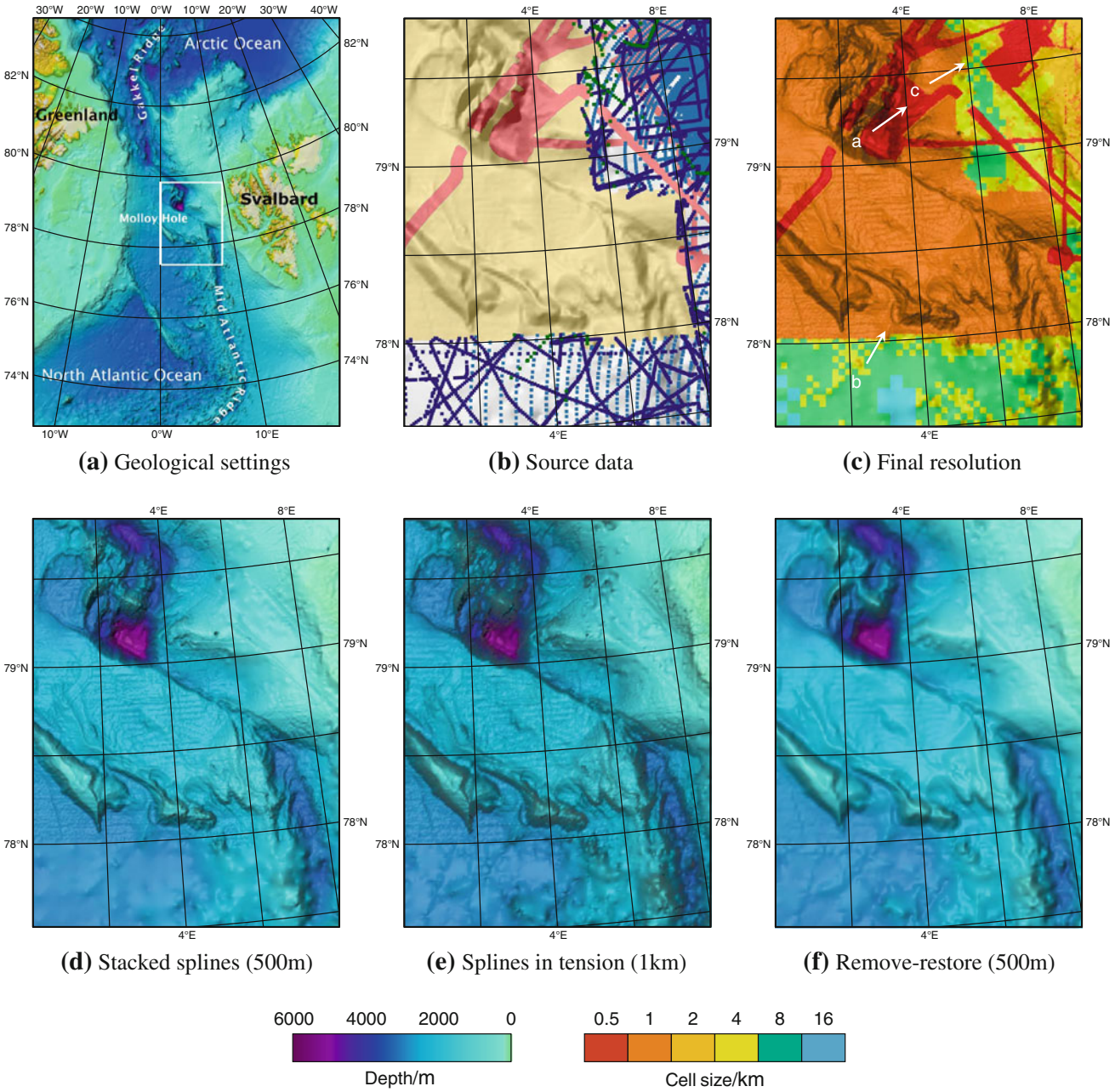

(a) Geological settings **(b)** Source data **(c)** Final resolution

(d) Stacked splines (500m) **(e)** Splines in tension (1km) **(f)** Remove-restore (500m)

Fig. 2 Comparison of various spline interpolation based gridding methods, using an identical source data set (**b**), comprising 100 m and 1 km multibeam grids (*red* and *yellow*, respectively), single beam soundings (*blue*) as well as submarine measurements (*green*). The results differ in the level of preserved small morphological details, the amount of artifacts at insufficiently constrained places or data set edges, and the overall smoothness of the grids. *Stacked splines* in tension allow for the highest resolution grids of all these methods, suppress artifacts well and yield a visually pleasing surface. The effective resolution of the *stacked splines grid* (**c**) closely follows the source data density. The *arrows* in (**c**) indicate location and direction of the detailed views in Fig. 3

(Jakobsson et al. 2008). These data include high-resolution multibeam measurements processed to 100 m × 100 m grids and a 1,000 m × 1,000 m grid, dense single beam echo sounding tracks from hydrographic surveys, and sparse tracks from individuals research cruises and submarines (Fig. 2b). The complete data set is made up of 492,106 depth samples in total of which 11,972 are single beam echo soundings and 480,134 from the multibeam based grid nodes. The 100 m × 100 m multibeam grids cover 13 percent of the total area while the 1,000 m × 1,000 m multibeam grid covers 61 percent. The southern part of the area is only mapped with sparse data and there are regions more than 5 km away from the closest source data point.

The positions are given in projected polar stereographic coordinates. Nevertheless, *surface* could correctly compute the necessary distance calculations for geographic coordinates as well.

Results

Figure 2 shows the results from gridding a sample data set of soundings with different spline interpolation based methods. The stacked splines grid was obtained with our method as described above. The output grid has a constant cell size grid of 500 m, and a grid with the resolution factor *n* for each grid cell was produced as a bi-product (Fig. 2c). The remove-restore grid was obtained in the same way as implemented by Becker et al. (2009), based on this groups scripting of GMT routines (D. Sandwell, pers. comm.). The grid also has a cell size of 500 m. As low-frequency field the first version of IBCAO was used (Jakobsson et al. 2000). IBCAO v1 features a cell size of 2.5 km and its source data do not include the more recent multibeam surveys. The splines in tension grid is obtained following the procedure by (Smith and Wessel 1990), with the same tension factor as used for the stacked splines method,

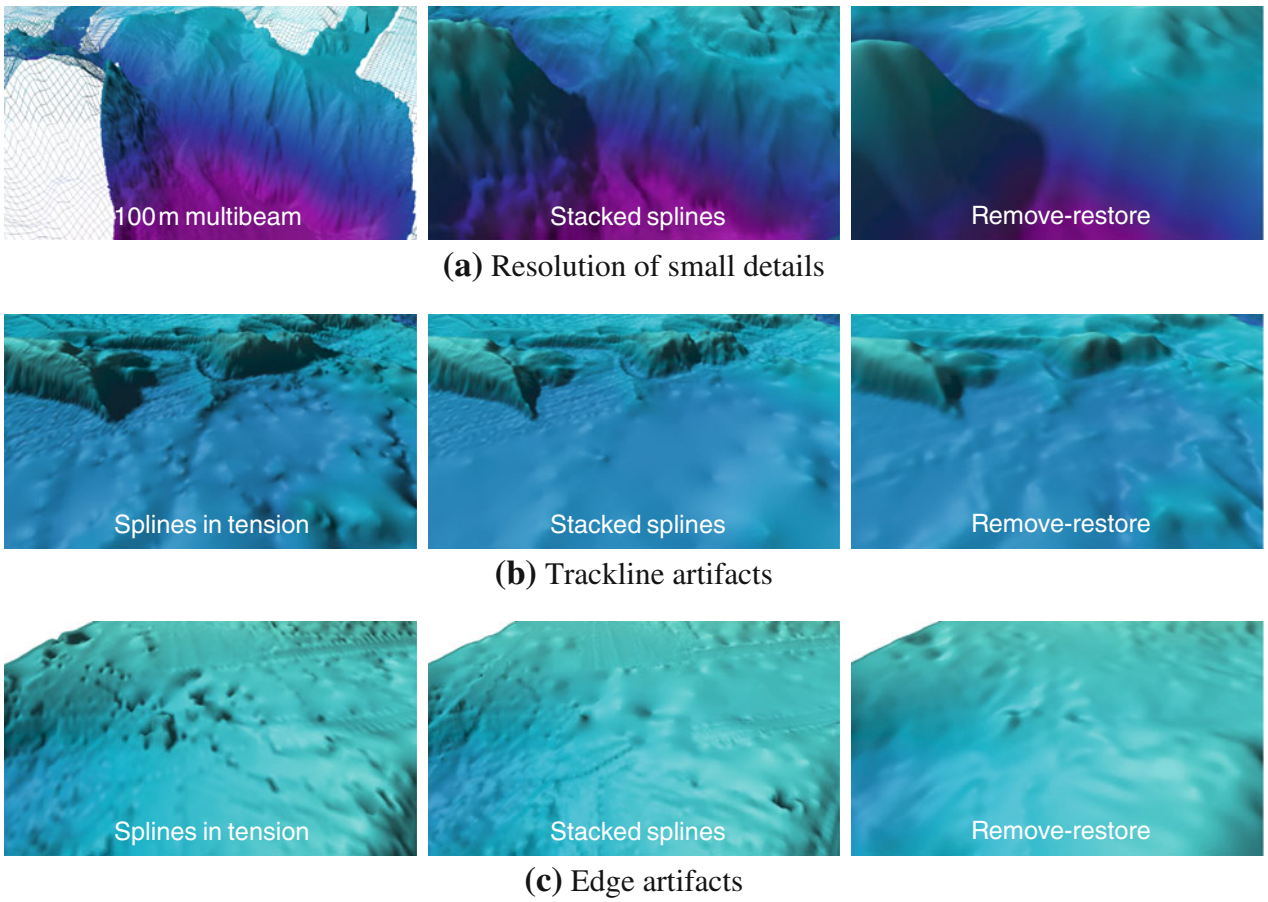

Fig. 3 In their details, the three compared grids vary significantly. The *stacked splines grid* preserves a lot of small morphological features from the source data, which are lacking in the *remove-restore* results (**a**). Both the *remove-restore* and the *stacked splines* approach give pleasing results in areas with sparse source data, where *splines in tension* develop distracting track line artifacts (**b**). With regard to artifacts around the edges of high-resolution source data, the *remove-restore* method is most capable of all three, although at the cost of small details (**c**). *Splines in tension* are prone to large bumps and spikes in areas with highly variable source data density (**c**). Postions and directions of the views as indicated in Fig. 2c

$T = 0.32$. This grid features a grid cell size of 1 km, as higher resolution interpolation resulted in deterioration of the result due to severe artifacts.

Overall, the remove-restore grid (Fig. 2f) looks cleanest with regard to gridding artifacts, whereas the splines in tension grid (Fig. 2e) shows a lot of artifacts in areas with sparse source data. However, the remove-restore grid contains a lot less small morphological details than the two other grids and it looks smooth as if it was low pass filtered. The stacked splines grid (Fig. 2d) appears most balanced with regard to small details and few artifacts.

A closer examination of details in the grids (Fig. 3) leads to a number of results. Even though the level of detail present in the high-resolution source data (Fig. 3a left) cannot be preserved during subsampling by a factor of five, the lack of details of the remove-restore grid (right) is striking in comparison to stacked splines (middle) or splines in tension (not shown). In terms of small details, gridding with stacked splines and splines in tension gives similar results at similar grid resolutions, but stacked splines may allow for a higher grid resolution resolving details better.

The possible grid resolution of splines in tension interpolation is limited by the appearance of artifacts around data points in areas with sparse source data (Fig. 3b). These artifacts appear mostly because the curvature of the surface focuses around the supporting data points. To a lesser extent, remove-restore is also affected from such artifacts. In the common case of single beam measurements along ship tracks, these artifacts can become very obvious along track lines in the visualized grids, even though the amplitude of the artifacts is usually small. Stacked splines are less prone to such artifacts, since the effective grid resolution is lower in areas with such track lines, so that the block median subsampling achieves a data distribution without strongly linearly ordered data points. Because of the lower effective grid resolution in these areas, a decrease in small details may be the trade-off for avoiding track line artifacts with stacked splines interpolation.

The remove-restore algorithm suppresses edge artifacts around high-resolution source data adjacent to areas with sparse data support very well, albeit at a loss of small details. In the stacked splines grid, such edges are visible, but comparatively smooth. In the case of the splines in tension grid, areas where many different source data sets overlap and the source data density varies a lot over small distances are characterized by severe holes and bumps. These problematic areas are portrayed much smoother by the stacked splines and remove-restore methods.

Because of the smoothness of the remove-restore grid, the spectral density of the grids was analyzed (Fig. 4). The comparison of the spectra clearly shows a much lower proportion of short wavelength signals in the remove-restore grid. Further testing is needed to exclude the possibility that this might be caused by an error in our implementation. The difference between the stacked splines and splines in tension grids is relatively small, and only present at short wavelengths. This difference is further discussed in the following section.

Discussion

At scales greater than a few hundred meters, because of the fractal character seafloor topography, its spectrum resembles that of Brownian noise (Bell 1979; Fox and Hayes 1985). Strictly speaking this applies only when staying within one geological setting, as an inhomogeneity component is introduced when different geological provinces are covered (Bell 1979). In a log-log plot of the spectral

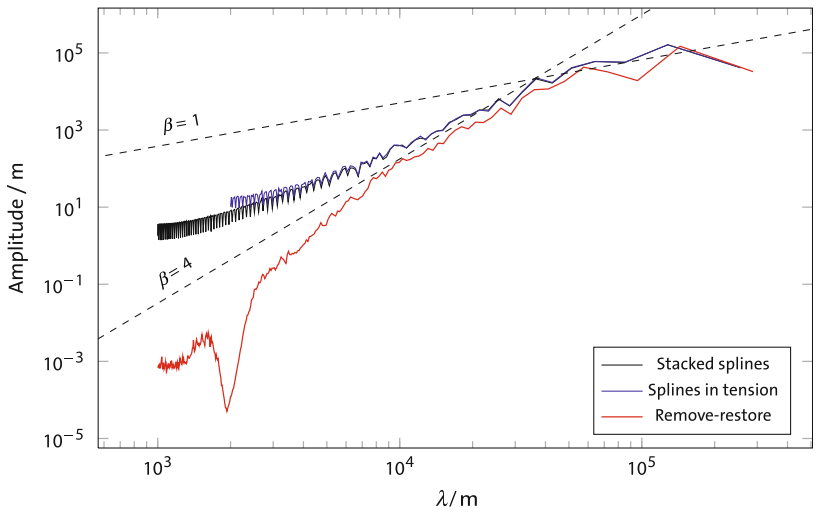

Fig. 4 Spectral density of the grids. At wavelengths larger than ca. 250 m, seafloor topography on the Earth follows the spectrum of Brownian noise, with a slope of $\beta = 1$ (see text). The spectrum of bicubic splines (without tension) are bound under a power law with exponent $\beta = 4$. Splines in tension lie between these two. The remove-restore grid shows surprisingly little high-frequency content

density this corresponds to a line with slope $\beta = 1$. Smith (1993) showed that the spectrum of a bicubic spline surface, however, is bound by a power law represented by $\beta = 4$. The spectrum of a surface interpolated with bicubic splines is a combination of the two, with $\beta = 4$ dominating at wavelengths shorter than the typical spacing of the source data. Adding tension to spline interpolation increases the short wavelength proportion of the solution, resulting in $1 < \beta < 4$ at short wavelengths.

The spectra of the surfaces interpolated with stacked splines and splines in tension appear to follow this relation, although the area is too small to draw conclusions about the longer wavelengths and to fit the power law lines more exactly. The largest gaps in our data set approximately have the size indicated by the intersection of the two lines for $\beta = 1$ and $\beta = 4$, i.e. ca. 20 km. The small loss in high frequency content of the stacked splines surface may be explained by the contributions of the grids with resolutions lower than 1 km, that is, the resolution of the splines in tension grid. The additional high-frequency contents in the splines in tension grid are probably mostly due to interpolation artifacts that are better suppressed in the stacked splines grid. What at first glimpse looks like a disadvantage of our method, may actually be an advantage.

In comparison to other spline interpolation based gridding methods, the stacked splines approach yields the most balanced result in terms of suppressing gridding artifacts while maintaining small details in the bathymetry. The method allows for adjusting the grid resolution to the highest resolution found in the source data, without the risk of introducing artifacts in badly constrained areas of the grid. The gridding is carried out at various resolutions, locally adapted to the source data density, and the output can be a grid with varying cell size.

As an extra benefit, the method can also provide a measure of source data density (Fig. 2c). Large compilations of bathymetric data often have to rely upon very heterogeneous source data sets. Such metadata may therefore convey valuable information e.g. about the expected data quality of the grid, or helps to explain whether or not a feature in the DBM might just be an artifact from the compilation process. In the data set shown here, for example, a strip of multibeam measurements in NWSE direction east of the Molloy Hole might be misinterpreted as a morphological feature of geologic origin. However, the comparison with the effective grid resolution reveals this trace as a source data related artifact in the grid.

One major advantage of the stacked splines approach is the possibility to increase gridding resolution without the risk of negative side effects in the form of gridding artifacts. This improves the ability of resolving small details in the seafloor morphology even for regional DBM compilations, where areas with only sparse data support can often not be avoided.

Conclusions

In this work, a refined approach for gridding with minimum curvature splines in tension at multiple grid resolutions has been developed. Stacked splines in tension provide a possibility to obtain grids with varying grid cell size, where the local data density in and around each grid cell determines the grid cell size.

Especially in areas with sparse source data in the form of single beam lines, track line artifacts could be reduced significantly in comparison to gridding with splines in tension. At the same time, small details in the seafloor morphology are preserved better than with the remove-restore approach. Gridding with stacked splines allows for a higher grid resolution, which can be determined by the areas with the highest source data density, without becoming unstable in less well-constrained areas with regard to unwanted gridding artifacts. Overall, the method offers a good balance between resolving power in well-mapped areas and stability where data is sparse.

The trade-off is higher computational requirements, as the gridding of the source data set has to be carried out multiple times. However, the finite difference algorithm used in GMT surface to numerically solve the differential equation for bicubic splines in tension are very efficient, and our tests were in no way limited by the computational power of even an ordinary desktop computer.

Acknowledgements David Sandwell provided the shell scripts for the remove-restore method. We are grateful for the valuable comments on the manuscript by Paul Wessel and another anonymous reviewer.

References

Becker JJ, Sandwell DT, Smith WHF, Braud J, Binder B, Depner J, Fabre D, Factor J, Ingalls S, Kim SH, Ladner R, Marks K, Nelson S, Pharaoh A, Trimmer R, von Rosenberg J, Wallace G, Weatherall P (2009) Global bathymetry and elevation data at 30 arc seconds resolution: Srtm30_plus. Mar Geod 32:355–371. doi:10.1080/01490410903297766

Bell TH Jr (1979) Mesoscale seafloor roughness. Deep Sea Res A 26(1):65–76. doi:10.1016/0198-0149(79)90086-4

de Boor C (2001) A practical guide to splines, applied mathematical sciences, vol 27. Springer, New York

Briggs IC (1974) Machine contouring using minimum curvature. Geophys 39:39–48

Burrough PA, McDonnel RA (1998) Principles of geographical information systems. Oxford University Press, Oxford

Delaunay B (1934) Sur la sphère vide. Bull Acad Sci USSR Classe Sci Mat Nat VII:793–800

Farr TG, Rosen PA, Caro E, Crippen R, Duren R, Hensley S, Kobrick M, Paller M, Rodriguez E, Roth L, Seal D, Shaffer S, Shimada J, Umland J, Werner M, Oskin M, Burbank D, Alsdorf D (2007) The shuttle radar topography mission. Rev Geophys 45(RG2004). doi:10.1029/2005RG000183

Forsberg R (1993) Modelling the fine-structure of the geoid: methods, data requirements and some results. Surv Geophys 14(4):403–418. doi:10.1007/BF00690568

Forsberg R, Tscherning C (1981) The use of height data in gravity field approximation by collocation. J Geophys Res 86(B9): 7843–7854. doi:10.1029/JB086iB09p07843

Fox CG, Hayes DE (1985) Quantitative methods for analyzing the roughness of the seafloor. Rev Geophys 23(1):1–48. doi:10.1029/RG023i001p00001

Furrer R, Genton MG, Nychka D (2006) Covariance tapering for interpolation of large spatial datasets. J Comput Graph Stat 15(3):502–523. doi:10.1198/106186006X132178

Haining RP, Kerry R, Oliver MA (2010) Geography, spatial data analysis, and geostatistics: an overview. Geogr Anal 42(1):7–31. doi:10.1111/j.1538-4632.2009.00780.x

Hall J (2006) GEBCO centennial special issue charting the secret world of the ocean floor: the GEBCO project 19032003. Mar Geophys Res 27(1):1–5. doi:10.1007/s11001-006-8181-4

Hartman L, Hössjer O (2008) Fast kriging of large data sets with gaussian markov random fields. Comput Stat Data Anal 52:2331–2349. doi:10.1016/j.csda.2007.09.018

Isaaks EH, Srivastava RM (1990) An introduction to applied geostatistics. Oxford University Press, Oxford

Jakobsson M, Cherkis N, Woodward J, Macnab R, Coakley B (2000) New grid of Arctic bathymetry aids scientists and mapmakers. EOS Trans 81(9):89, 93 & 96

Jakobsson M, Macnab R, Mayer L, Anderson R, Edwards M, Hatzky J, Schenke HW, Johnson P (2008) An improved bathymetric portrayal of the Arctic Ocean: implications for ocean modeling and geological, geophysical and oceanographic anlyses. Geophys Res Lett 35:L07,602. doi:10.1029/2008GL033520

Klenke M, Schenke HW (2002) A new bathymetric model for the central fram strait. Mar Geophys Res 23(4):367–378. doi:10.1023/A:1025764206736

Macnab R, Jakobsson M (2000) Something old, something new: compiling historic and contemporary data to construct regional bathymetric maps, with the Arctic Ocean as a case study. Int Hydrogr Rev 1(1):2–16

Matheron G (1963) Principles of geostatistics. Econ Geol 58:1246–1266

Müller RD, Sdrolias M, Gaina C, Roest WR (2008) Age, spreading rates, and spreading asymmetry of the world's ocean crust. Geochem Geophys Geosyst 9(4):Q04,006. doi:10.1029/2007GC001743

Pollard JM (1971) The fast fourier transform in a finite field. Math Comput 25(114):365–374

Reuter H, Nelson A, Jarvis A (2007) An evaluation of void filling interpolation methods for srtm data. Int J Geogr Inf Sci 21(9): 983–1008

Sandwell DT, Smith WHF (1997) Marine gravity anomaly from Geosat and ERS 1 satellite altimetry. J Geophys Res 102:10039–10054

Smith WHF (1993) On the accuracy of digital bathymetric data. J Geophys Res 98(B6):9591–9603

Smith WHF, Sandwell DT (1997) Global sea floor topography from satellite altimetry and ship depth soundings. Science 277:1956–1962

Smith WHF, Wessel P (1990) Gridding with continuous curvature splines in tension. Geophys 55(3):293–305

Task group on gridding of the GEBCO SCDB (1997) On the preparation of a gridded data set from the GEBCO Digital Atlas contours. Tech. rep., GEBCO, version 9–16 June 1997

Tobler W (1970) A computer movie simulating urban growth in the detroit region. Econ Geogr 46:234–240

Torge W (2001) Geodesy. De Gruyter, 281ff

Vogt PR, Jung WY, Nagel DJ (2000) GOMaP: a matchless resolution to start the new millennium. EOS Trans 81(23):254, 258

Ware C (1989) Fast note: fast hill shading with cast shadows. Comp Geosci 15(8):1327–1334

Wessel P, Smith WHF (1998) New, improved version of generic mapping tools released. EOS Trans 79(47):579

Zhou Q, Liub X (2004) Analysis of errors of derived slope and aspect related to dem data properties. Comp Geosci 30(4):369–378. doi:10.1016/j.cageo.2003.07.005